Optica Applicata, Vol. LII, No. 4, 2022
DOI: 10.37190/oa220412

Controllable propagation of Pearcey–Gaussian beams in photorefractive media with fractional Schrödinger equation

Teng Guo, Ru Gao, Shumin Ren, Pengxiang Wang, Yan Xiao*

College of Physics and Electronics Engineering, Shanxi University, Taiyuan 030006, China

*Corresponding author: xiaoyan@sxu.edu.cn

Taking the fractional Schrödinger equation as the theoretical model, the evolution behavior of the Pearcey–Gaussian beam in the photorefractive medium is studied. The results show that breathing solitons are generated when the nonlinear effect and the diffraction effect are balanced with each other. Nonlinear coefficients, Lévy index and beams amplitude affect breathing period of the soliton and maximum peak intensity. Within a certain range, the breathing period of the soliton decreases with the increase of the nonlinear coefficient and the Lévy index. However when the beams amplitude increases, the breathing period and the maximum peak intensity of the soliton increase. Under the photorefractive effect, due to the bidirectional self-acceleration property of the Pearcey beam, the solitons formed will propagate vertically. These properties can be used to manipulate the beam and have potential applications in optical switching, plasma channeling, particle manipulation, *etc*.

Keywords: Pearcey–Gaussian beam, fractional Schrödinger equation, photorefractive media, breathing soliton.

1. Introduction

In 2007, Anguiano-Morales group proposed and experimentally obtained a diffraction-free caustic beam [1], and pointed out that the caustic beam has self-healing properties [2]. In 2015, Vaveliuk *et al*. divided the caustic beam into two types: folded caustic beam and tip caustic beam according to the symmetry of the spectral phase [3]. The representative of folded caustic beam is Airy beam [4], which has the characteristics of self-acceleration [5], non-diffraction [6] and self-healing [7–9]. So these properties have a wide application prospect in particle removal [10–12], biomedical treatment [13], optical imaging [14, 15] and so on. Pearcey beam, as a representative of tip caustic beam, has been studied extensively by researchers. In 2012, researchers experimentally obtained a new kind of beam, called the Pearcey beam, which based on the Pearcey function [16], it was proved that the Pearcey beam exhibits similar prop-

erties to Airy beam and Bessel beam, and it is proved that the Pearcey beam has self -focusing and self-healing properties [17]. DENG *et al*. studied the virtual light source problem of the Pearcey beam [18]. Later, KOVALEV *et al*. generated the half-Pearcey beam and found that the Pearcey beam was formed by the interference of two half -Pearcey beams [19]. In 2016, BOUFALAH *et al*. studied the influence of atmospheric turbulence on the transmission of Pearcey beams [20]. At the same time, the study also found that Pearcey beam is a beam of unchanging form, which is very similar to Gaussian beam [21]. With the change of transmission distance, the light field distribution is also changing, but it can always be expressed by the Pearcey function.

The fractional Schrödinger equation, as a linear partial differential equation, was first proposed by LASKIN in 2000, and research at the time focused on the mathematical issue [22–24]. Until 2015, LONGHI introduced the fractional Schrödinger equation into the field of optics [25], which attracted widespread attention, and then based on the fractional Schrödinger equation model, the transmission properties of Airy beams [26], Gaussian beams [27] and super-Gaussian beams [28] were discussed, and the PT symmetric potential [29], linear potential [30] and other media had been widely studied. Photorefractive medium [31–33] is a nonlinear medium that produces photoreceptive refractive index changes. The input beam excites the carriers formed by impurities or defects, generating a photosensitive electric field, which causes the refractive index of the medium to change, and solitons are obtained by the balance between the diffraction effect and the nonlinear effect. In recent years, solitons have drawn extensive research by scholars; in 2009, the soliton solution of the NLSE was obtained in various forms of non-Kerr law media [34]. Furthermore, the complex cubic-quintic Ginzburg–Landau equation (CCQGLE) was also a common theoretical model. Analytic one-soliton solution for the variable coefficients CCQGLE was constructed by researchers [35]. Subsequently, the research team obtained the bright, dark and singular soliton solutions by theoretically solving the coupled Fokas–Lenells equation [36,37]. Additionally, highly dispersive optical solitons were discussed by F-expansion scheme in 2018 [38]. These studies provide a theoretical basis for the stable transmission of optical fiber communication.

Based on the fractional Schrödinger equation, the propagation properties of Pearcey –Gaussian beams in photorefractive media are discussed by numerical simulation. By changing beam parameters and medium parameters, including beam amplitude, distribution factor, Lévy index, and nonlinear coefficient, the diffraction effect of the beam is balanced by the nonlinear effect of the medium, which controls the formation and the transmission of the solitons. Due to unique optical characteristics of the Pearcey beam, it has broad application prospects in optical trapping and particle capture.

2. Theoretical model

Under the paraxial approximation, taking the fractional Schrödinger equation as the theoretical model, the dynamic equation of beam propagation in the photorefractive medium:

$$i\frac{\partial}{\partial Z}\Phi(X,Z) = \frac{1}{2}\left(-\frac{\partial^2}{\partial X^2}\right)^{\alpha/2}\Phi(X,Z) + \beta\frac{\Phi(X,Z)}{1+|\Phi(X,Z)|^2} \tag{1}$$

where $\Phi(X, Z)$ is the dimensionless slowly varying envelope of the light beam; $X = x/x_0$ and $Z = z/kx_0^2$ are the normalized transverse coordinate and propagation distance, respectively; x_0 is the transverses characteristic width; kx_0^2 is the Rayleigh length; $k = k_0 n_e = (2\pi/\lambda_0)n_e$, λ_0 is the free space wavelength, n_e is the extraordinary refractive index; α ($1 \le \alpha \le 2$) is the Lévy index, when $\alpha = 2$ it is the standard nonlinear Schrödinger equation; β represents the nonlinear coefficient, $\beta = (k_0 x_0)^2(n_e^4\gamma_{33}/2)E_0$, where γ_{33} is the electro-optical coefficient and E_0 is the external electric field.

The light field distribution of the initially incident Pearcey–Gaussian beam:

$$\Phi(X, 0) = A_0\,\mathrm{Pe}(X)\exp(-\chi_0^2 X^2) \tag{2}$$

where A_0 is the amplitude of the incident beam, $\mathrm{Pe}(X) = \int_{-\infty}^{+\infty} \mathrm{d}s \exp[i(s^4 + sX)]$ is the Pearcey function, and χ_0 is the distribution factor.

3. Numerical simulation

Using the split-step Fourier method, the Pearcey–Gaussian beam is used as the incident beam to study its propagation characteristics in the photorefractive medium.

Figure 1 shows the propagation evolution diagram of the Pearcey–Gaussian beam in the photorefractive medium with different distribution factor χ_0 and nonlinear co-

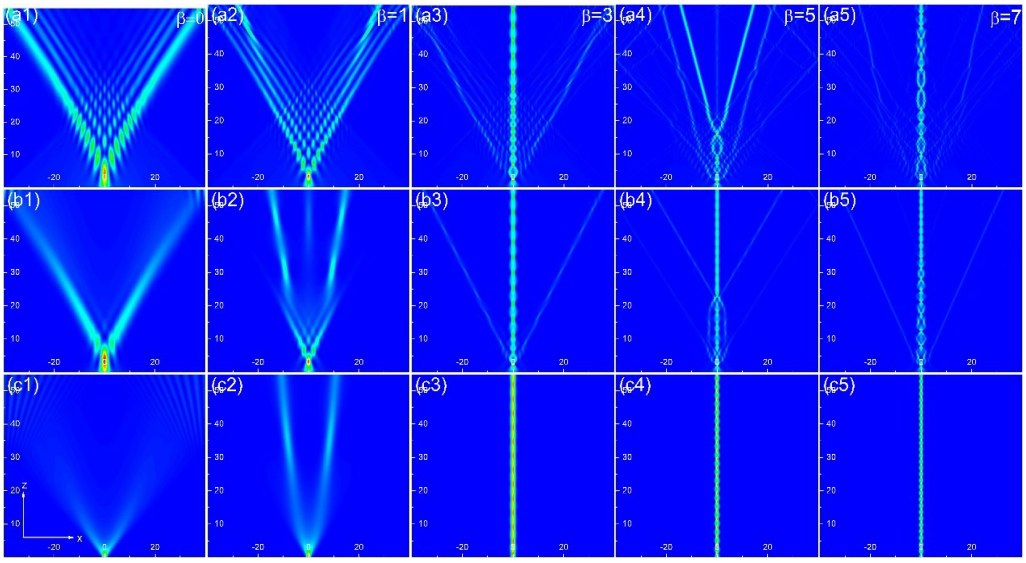

Fig. 1. Propagation evolution diagram of the Pearcey–Gaussian beam in photorefractive medium with different χ_0 when $A_0 = 2$, $\alpha = 1.5$, and $\beta = 0$ (a1–c1), $\beta = 1$ (a2–c2), $\beta = 3$ (a3–c3), $\beta = 5$ (a4–c4), $\beta = 7$ (a5–c5); (a1–a5) $\chi_0 = 0.01$, (b1–b5) $\chi_0 = 0.1$, and (c1–c5) $\chi_0 = 0.9$.

efficient parameter β. In Fig. 1(a1), when $\beta = 0$, coherent diffraction occurs in the Pearcey beam, resulting in fish-scale phenomenon. When the effect of nonlinear media is not considered, due to the bidirectional self-acceleration property of the Pearcey beam, as the propagation distance increases, the Pearcey beam will split and propagate to both sides. In Fig. 1(a3), when $\beta \neq 0$, as the increase of β, the nonlinear effect of the medium and the diffraction of the beam reach a preliminary balance, and the main lobe beam forms a soliton. With the growing of the nonlinear coefficient β, and the nonlinear effect of the medium gradually increasing, the beam behaves as a bound state, and the sidelobe beam is continuously reduced, and the energy starts to converge toward the middle (see Fig. 1(a4–a5)). In Fig. 1(b3), when $\beta = 3$, the self-focusing effect of the medium and the diffraction effect of the beam are further enhanced, and the solitons formed are more stable during the transmission. In Fig. 1(b4) and (b5), as β increases, the breathing period and amplitude of the breathing soliton become smaller, and the energy of the sidelobe gradually transfers to the main beams, and the energy of the sidelobe becomes smaller and smaller. In Fig. 1(a1), (b1), (c1), when $\beta = 0$, the distribution factors χ_0 are 0.01, 0.1, and 0.9, respectively, and with the increase of χ_0, the beam diffraction speed is faster and the energy decays rapidly. When the nonlinear coefficient is a certain value, the larger the χ_0 is, the less the side lobes of the beam will be, and the energy of the main lobe will be more concentrated. Thus, it is easy to form a stable soliton (see Fig. 1(a3), (b3), (c3)). Therefore, only nonlinear coefficients β in a certain range can form breathing solitons, too large or too small, and it will be difficult to form stable solitons, while the light field distribution factor χ_0 also has a certain influence on the formation of solitons.

Figure 2 describes the influence of different nonlinear coefficients β and Lévy index α on the transmission characteristics of the Pearcey–Gaussian beam. When the Lévy index α and the nonlinear coefficient β are both small, there are soliton-like generations, as shown in Fig. 2(a1). In Fig. 2(a2–a4), with the increase of Lévy index α, and the diffraction effect which is greater than the nonlinear effect, it is difficult to form a spatial soliton. In Fig. 2(b1, b2), as the nonlinear coefficient rises, at this time, the nonlinear effect and the diffraction effect of the beam are balanced with each other, and breathing solitons are generated. With the increase of the Lévy index α, the diffraction effect of the beam is gradually stronger than the nonlinear effect of the medium, and the stability of the spatial soliton becomes worse (see Fig. 2(b3, b4)). In Fig. 2(c1, c2) and (d1, d2), breathing solitons are generated during the transmission process and present a stable breathing state with the growing of the β. In Fig. 2(c3, c4), three soliton beams are formed. Due to the bidirectional self-acceleration behavior of the Pearcey beam, the middle soliton always steadily propagates along the Z axis, while the two solitons are separated from each other. As the Lévy index α increases, the breathing period of the soliton becomes smaller. In Fig. 2(d3, d4), there are also three solitons formed, and as α increases, the breathing amplitude of the soliton will also increase. As β further increases, the nonlinear effect of the medium is stronger than the diffraction effect of the beam, the beam converges more obviously, and the breathing period and amplitude of the soliton gradually become smaller (see Fig. 2(b3), (c3), (d3)).

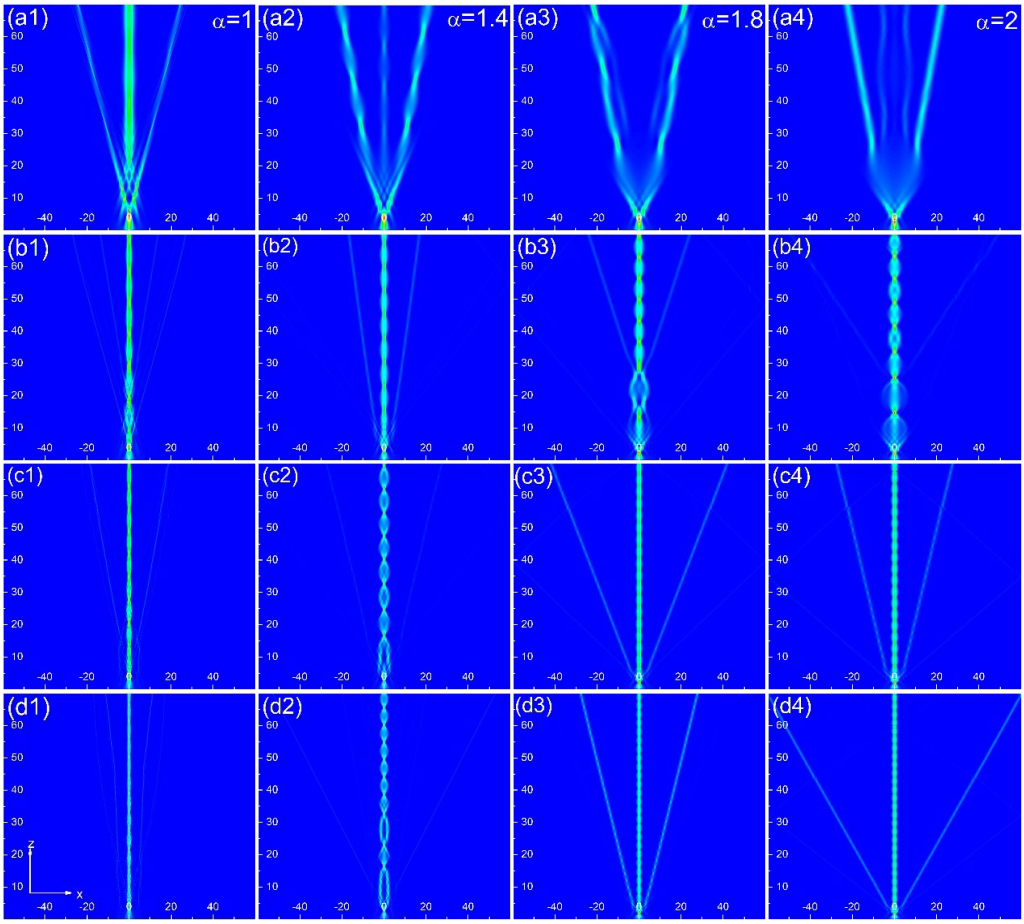

Fig. 2. The evolution of the Pearcey–Gaussian beam in photorefractive media with different α when $A_0 = 2$, $\chi_0 = 0.1$, and $\beta = 1$ (a1–a4), $\beta = 3$ (b1–b4), $\beta = 5$ (c1–c4), $\beta = 7$ (d1–d4); (a1–d1) $\alpha = 1$, (a2–d2) $\alpha = 1.4$, (a3–d3) $\alpha = 1.8$, and (a4–d4) $\alpha = 2$.

These characteristics can be used to control the beam transmission, which has potential application value in optical switch, splitter and other fields.

In order to further observe the characteristics of the breathing solitons during the transmission of the beam, Fig. 3 shows the waveform diagram of the Pearcey–Gaussian beam at different transmission distances when the nonlinear coefficient β is 3, 5, and 7, respectively. Figures 3(a), (b), (c) correspond to Fig. 2(b4), (c4), (d4). From Fig. 3(a), we can clearly see the complete breathing process of the spatial soliton. When $\beta = 3$, the beam will form a stable breathing soliton during the transmission, and the lateral width of the main lobe shows periodic changes as the transmission distance increases. When $\beta = 5$ and $\beta = 7$, as shown in Fig. 5(b) and (c), there are symmetrical side lobes on both sides of the main lobe. As the nonlinear coefficient β increases, the breathing period of the spatial soliton becomes smaller, which is consistent with the phenomenon

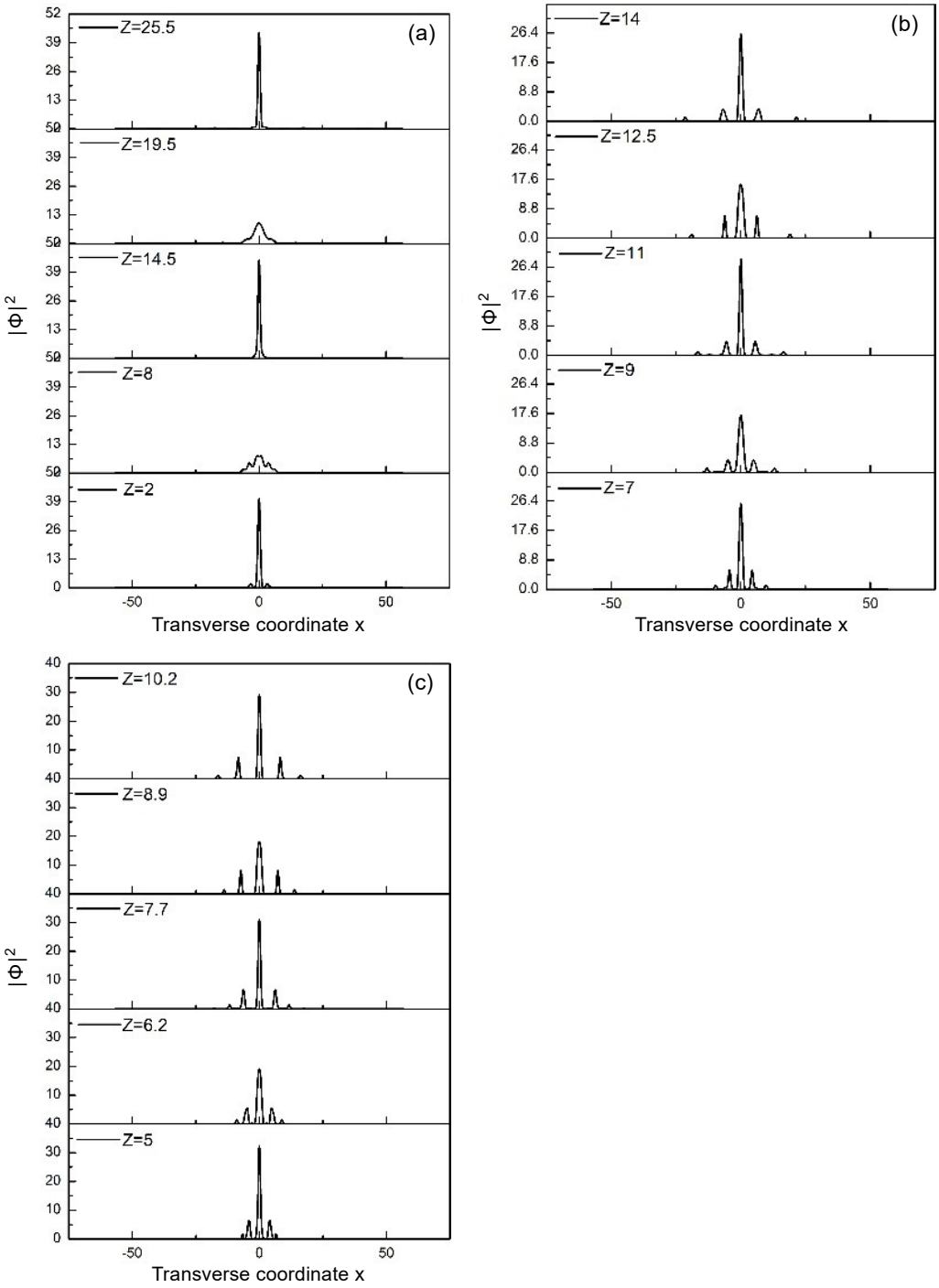

Fig. 3. Transmission waveforms of Pearcey–Gaussian beams at different transmission distances when $A_0 = 2$, $\chi_0 = 0.1$, $\alpha = 2$ and β are set at different values: (a) $\beta = 3$, (b) $\beta = 5$, and (c) $\beta = 7$.

in Fig. 2(b4), (c4) and (d4). It can be concluded that within a certain range, the larger the nonlinear coefficient β, the easier to form solitons, and the smaller the breathing period of the spatial soliton. This is in full agreement with the conclusion obtained in Fig. 2.

Figure 4 shows the propagation evolution of Pearcey–Gaussian beams in photorefractive media with different photorefractive coefficient β and beam amplitude A_0. The greater the beam amplitude A_0, the greater the initial incident power. In Fig. 4(a1–a4), when β is small, due to the weaker nonlinear effect, the increases of the amplitude will not generate soliton. In Fig. 4(b1–b4), when $\beta = 3$, due to the interaction between the nonlinear effect of the medium and the diffraction effect of the beam, there is a soliton shedding phenomenon. As A_0 increases, the breathing period of the soliton also becomes larger, the sidelobe energy continues to increase, and the energy of the main -lobe beam continues to decrease. In Fig. 4(b2), (c2), (d2), retaining A_0 unchanged,

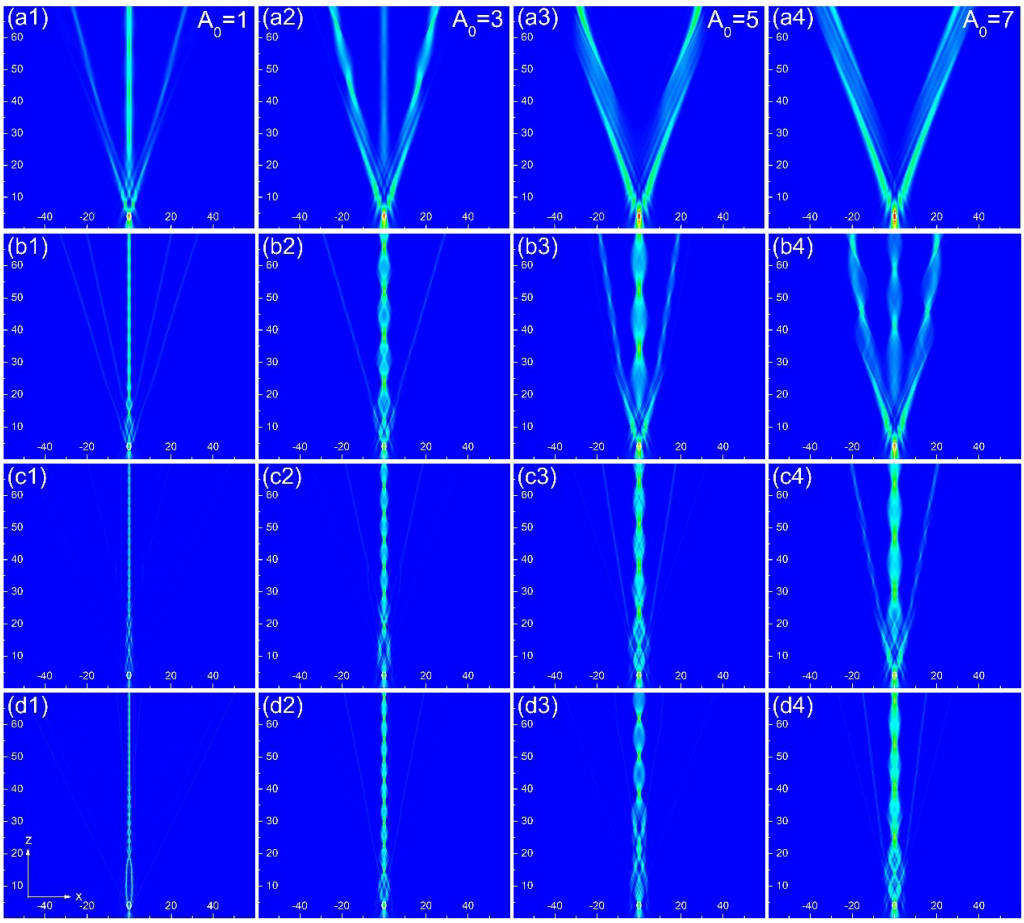

Fig. 4. The evolution of the Pearcey–Gaussian beam in photorefractive media with different A_0 when $\alpha = 1.2$, $\chi_0 = 0.1$, and $\beta = 1$ (a1–a4), $\beta = 3$ (b1–b4), $\beta = 6$ (c1–c4), $\beta = 9$ (d1–d4); (a1–d1) $A_0 = 1$, (a2–d2) $A_0 = 3$, (a3–d3) $A_0 = 5$, and (a4–d4) $A_0 = 7$.

with the increase of the nonlinear coefficient β, the formed breathing solitons are more stable, and the breathing period of the soliton becomes smaller. In short, the beam amplitude A_0 has a certain influence on the formation of breathing solitons, and within a certain amplitude range, stable breathing solitons will be produced. In addition, the threshold range of this amplitude to form solitons will change as the nonlinear coefficient changes. Therefore, adjusting the beam amplitude A_0 and the nonlinear coefficient β can control the beam transmission.

In order to better show the evolution process of the soliton, Fig. 5 shows the relationship between the peak intensity of breathing soliton and the transmission distance with different nonlinear coefficients β, Lévy index α, and amplitude A_0. The periodic oscillation curve shows the formation of a stable breathing soliton during the transmission. In Fig. 5(a), as β increases, the transmission distance formed the soliton increases, and the soliton breathing period decreases. In Fig. 5(b), the breathing period of the soliton will decrease with the increase of α, and the state of the soliton becomes more stable. The maximum peak intensity of the breathing soliton will increase with the increase of A_0, and the transmission distance which formed the soliton also increases,

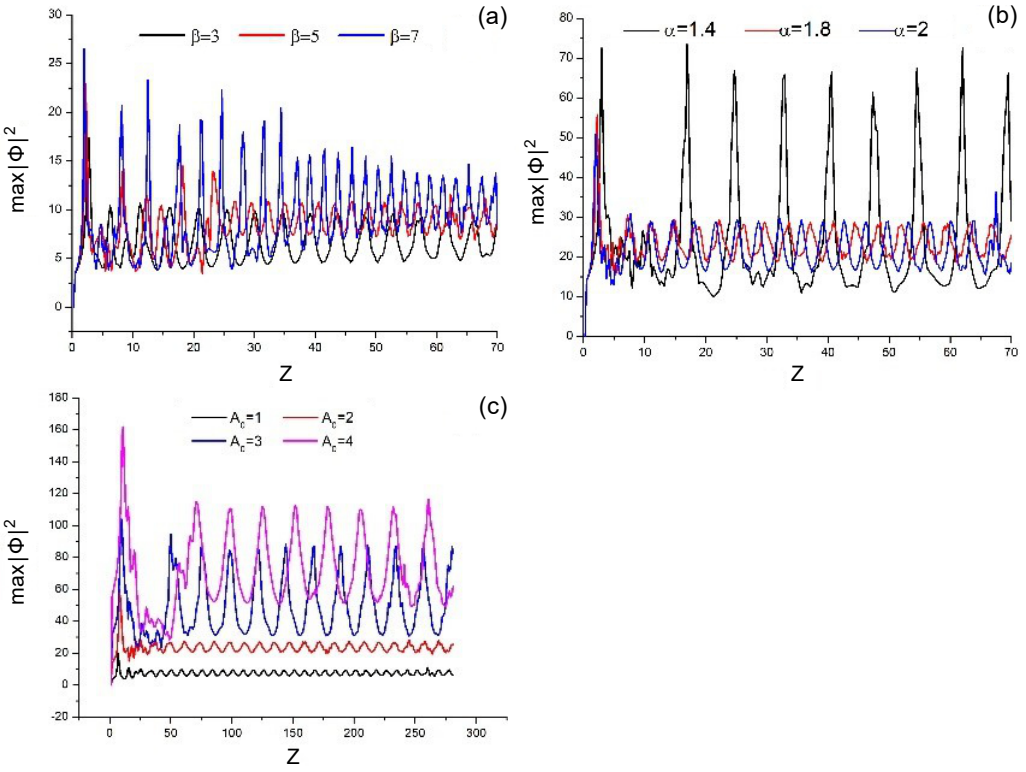

Fig. 5. Relationship between maximum peak intensity and propagation distance of shedding breathing solitons in Pearcey–Gaussian beams: (a) $\chi_0 = 0.1$, $A_0 = 1$, $\alpha = 1.5$, the photorefractive coefficients β are 3, 5, and 7; (b) $\chi_0 = 0.1$, $A_0 = 2$, $\beta = 5$ the Lévy index α are 1.4, 1.8, and 2; (c) $\chi_0 = 0.1$, $\beta = 6$, $\alpha = 1.8$ the amplitudes A_0 are 1, 2, 3, and 4.

and the period of the breathing soliton becomes larger (see Fig. 5(c)). The analysis results are consistent with the previous conclusions.

Figure 6 shows the transmission evolution of the Pearcey–Gaussian beam in the photorefractive medium with different Lévy index and beam amplitudes. In Fig. 6(a1–a4), when α is small, the beam state at this time is a bound state. When the Lévy index α increases, the diffraction effect of the beam is enhanced, new side lobes are continuously generated, and the breathing period of the space soliton is getting smaller and smaller (see Fig. 6(b2), (c2), (d2)). In Fig. 6(b2–b4), as A_0 increases, the nonlinear effect and the diffraction effect reach a balance, so the generation of breathing solitons can be observed. In Fig. 6(c3), the balance effect is further enhanced, and the formed breathing soliton is more stable. When the beam amplitude A_0 further increases, it can be found that the previous balance state begins to break. In this case, although there

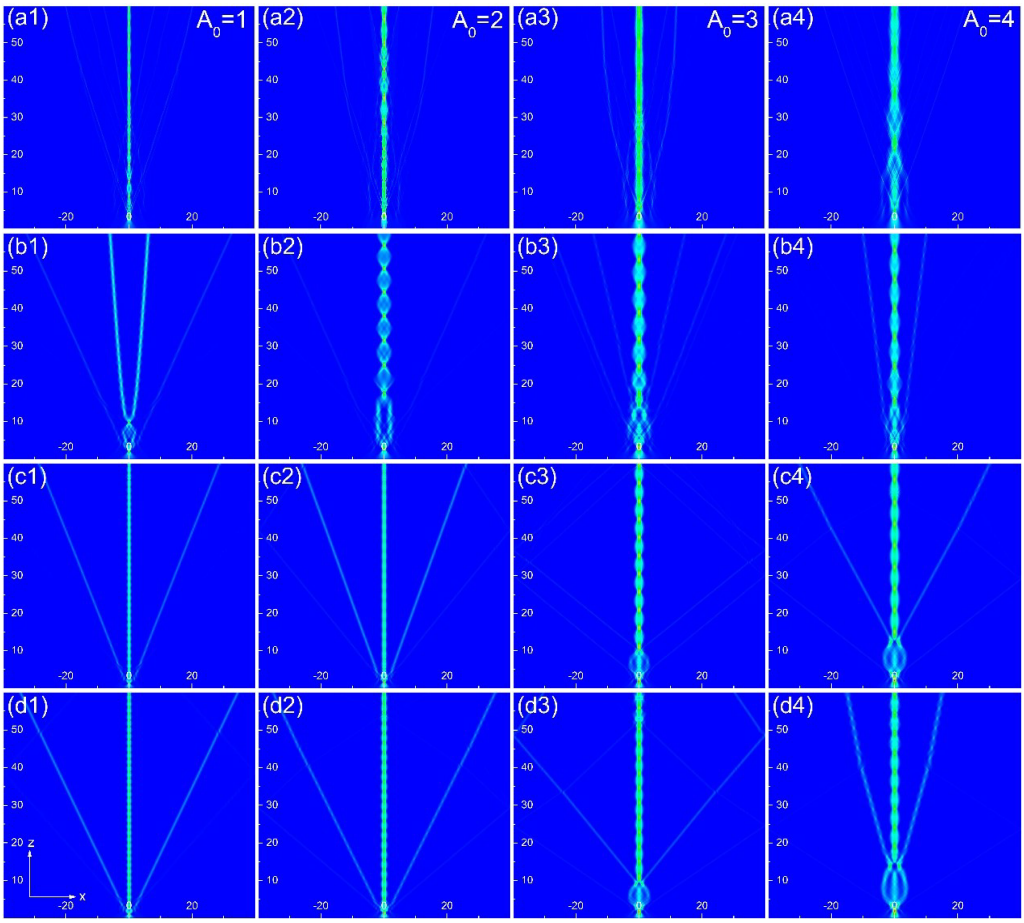

Fig. 6. The evolution of the Pearcey–Gaussian beam in photorefractive media with different α when $\beta = 6$, $\chi_0 = 0.1$, and $A_0 = 1$ (a1–d1), $A_0 = 2$ (a2–d2), $A_0 = 3$ (a3–d3), $A_0 = 4$ (a4–d4); (a1–a4) $\alpha = 1$, (a2–d2) $\alpha = 1.4$, (a3–d3) $\alpha = 1.8$, and (a4–d4) $\alpha = 2$.

are relatively stable breathing solitons, it can be clearly seen that the energy of the main lobe and the side lobe is divergent (see Fig. 6(c4)). In Fig. 6(d1–d4), with the increase of the amplitude A_0, the transmission distance formed the soliton and the breathing period of the soliton becomes larger, and the maximum lateral width of the soliton becomes larger.

4. Conclusion

Taking the fractional Schrödinger equation as the theoretical model, the propagation characteristics of the Pearcey–Gaussian beam in the photorefractive medium are numerically simulated. It is found that spatial solitons will be formed during the transmission, and the nonlinear coefficient β, the Lévy index α, the beam amplitude A_0 and the distribution factor χ_0 will have an important impact on the generation and transmission of spatial solitons. As the nonlinear coefficient β increases, spatial solitons will be formed during the transmission. When the nonlinear coefficient β increases to a certain value, the soliton will be more stable and can transmit stably along the Z-axis direction, and the breathing period and breathing amplitude of the soliton will also become smaller. The larger the is the distribution factor χ_0, the closer the beam distribution is to the Gaussian distribution, and the easier it is to form solitons. The amplitude A_0 also has a certain influence on the formation of breathing solitons. If the amplitude is too large or too small, no solitons can be generated, stable breathing solitons are formed only within a certain range. With the increase of the amplitude A_0, the transmission distance and breathing period of the soliton will also add. In addition, with the increase of the Lévy index α, the beam diffraction effect is enhanced, the breathing period of the soliton is reduced, and the breathing rate is accelerated. The conclusion shows that the transmission of the Pearcey–Gaussian beam is controllable, which provides a potential application value in optical signal processing.

References

[1] ANGUIANO-MORALES M., MARTÍNEZ A., ITURBE-CASTILLO M.D., CHÁVEZ-CERDA S., ALCALÁ-OCHOA N., *Self-healing property of a caustic optical beam*, Applied Optics **46**(34), 2007, pp. 8284–8290, DOI: 10.1364/AO.46.008284.

[2] ANGUIANO-MORALES M., *Transformation of Bessel beams by means of a cylindrical lens*, Applied Optics **48**(25), 2009, pp. 4826–4831, DOI: 10.1364/AO.48.004826.

[3] VAVELIUK P., LENCINA A., RODRIGO J.A., MATOS O.M., *Caustics, catastrophes, and symmetries in curved beams*, Physical Review A **92**(3), 2015, article no. 033850, DOI: 10.1103/PhysRevA.92.033850.

[4] BERRY M.V., BALAZS N.L., *Nonspreading wave packets*, American Journal of Physics **47**(3), 1979, pp. 264–267, DOI: 10.1119/1.11855.

[5] SIVILOGLOU G.A., BROKY J., DOGARIU A., CHRISTODOULIDES D.N., *Observation of accelerating Airy beams*, Physical Review Letters **99**(21), 2007, article no. 213901, DOI: 10.1103/PhysRevLett.99.213901.

[6] SIVILOGLOU G.A., CHRISTODOULIDES D.N., *Accelerating finite energy Airy beams*, Optics Letters **32**(8), 2007, pp. 979–981, DOI: 10.1364/OL.32.000979.

[7] BROKY J., SIVILOGLOU G.A., DOGARIU A., CHRISTODOULIDES D.N., *Self-healing properties of optical Airy beams*, Optics Express **16**(17), 2008, pp. 12880–12891, DOI: 10.1364/OE.16.012880.

[8] Chu X., Zhou G., Chen R., *Analytical study of the self-healing property of Airy beams*, Physical Review A **85**(1), 2012, article no. 013815, DOI: 10.1103/PhysRevA.85.013815.
[9] Cao R., Hua Y., Min C., Zhu S., Yuan X.-C., *Self-healing optical pillar array*, Optics Letters **37**(17), 2012, pp. 3540–3542, DOI: 10.1364/OL.37.003540.
[10] Baumgartl J., Mazilu M., Dholakia K., *Optically mediated particle clearing using Airy wavepackets*, Nature Photonics **2**, 2008, pp. 675–678, DOI: 10.1038/nphoton.2008.201.
[11] Christodoulides D.N., *Riding along an Airy beam*, Nature Photonics **2**, 2008, pp. 652–653, DOI: 10.1038/nphoton.2008.211.
[12] Baumgartl J., Hannappel G.M., Stevenson D.J., Day D., Gu M., Dholakia K., *Optical redistribution of microparticles and cells between microwells*, Lab on a Chip **9**(10), 2009, pp. 1334–1336, DOI: 10.1039/B901322A.
[13] Dasgupta R., Ahlawat S., Verma R.S., Gupta P.K., *Optical orientation and rotation of trapped red blood cells with Laguerre-Gaussian mode*, Optics Express **19**(8), 2011, pp. 7680–7688, DOI: 10.1364/OE.19.007680.
[14] Jia S., Vaughan J.C., Zhuang X., *Isotropic three-dimensional super-resolution imaging with a self-bending point spread function*, Nature Photonics **8**(4), 2014, pp. 302–306, DOI: 10.1038/nphoton.2014.13.
[15] Vettenburg T., Dalgarno H.I.C., Nylk J., Coll-Lladó C., Ferrier D.E.K., Čižmár T., Gunn-Moore F.J., Dholakia K., *Light-sheet microscopy using an Airy beam*, Nature Methods **11**, 2014, pp. 541–544, DOI: 10.1038/nmeth.2922.
[16] Pearcey T., *XXXI. The structure of an electromagnetic field in the neighbourhood of a cusp of a caustic*, The London, Edinburgh, and Dublin Philosophical Magazine and Journal of Science, Series 7 **37**(268), 1946, pp. 311–317, DOI: 10.1080/14786444608561335.
[17] Ring J.D., Lindberg J., Mourka A., Mazilu M., Dholakia K., Dennis M.R., *Auto-focusing and self-healing of Pearcey beams*, Optics Express **20**(17), 2012, pp. 18955–18966, DOI: 10.1364/OE.20.018955.
[18] Deng D., Chen C., Zhao X., Chen B., Peng X., Zheng Y., *Virtual source of a Pearcey beam*, Optics Letters **39**(9), 2014, pp. 2703–2706, DOI: 10.1364/OL.39.002703.
[19] Kovalev A.A., Kotlyar V.V., Zaskanov S.G., Porfirev A.P., *Half Pearcey laser beams*, Journal of Optics **17**(3), 2015, article no. 035604, DOI: 10.1088/2040-8978/17/3/035604.
[20] Boufalah F., Dalil-Essakali L., Nebdi H., Belafhal A., *Effect of turbulent atmosphere on the on-axis average intensity of Pearcey–Gaussian beam*, Chinese Physics B **25**(6), 2016, article no. 064208, DOI: 10.1088/1674-1056/25/6/064208.
[21] Deschamps G.A., *Gaussian beam as a bundle of complex rays*, Electronics Letters **7**(23), 1971, pp. 684–685, DOI: 10.1049/el:19710467.
[22] Laskin N., *Fractional quantum mechanics*, Physical Review E **62**(3), 2000, pp. 3135–3145, DOI: 10.1103/PhysRevE.62.3135.
[23] Laskin N., *Fractional quantum mechanics and Lévy path integrals*, Physics Letters A **268**(4–6), 2000, pp. 298–305, DOI: 10.1016/S0375-9601(00)00201-2.
[24] Laskin N., *Fractional Schrödinger equation*, Physical Review E **66**(5), 2002, article no. 056108, DOI: 10.1103/PhysRevE.66.056108.
[25] Longhi S., *Fractional Schrödinger equation in optics*, Optics Letters **40**(6), 2015, pp. 1117–1120, DOI: 10.1364/OL.40.001117.
[26] Huang X.W., Deng Z.X., Fu X.Q., *Dynamics of finite energy Airy beams modeled by the fractional Schrödinger equation with a linear potential*, Journal of the Optical Society of America B **34**(5), 2017, pp. 976–982, DOI: 10.1364/JOSAB.34.000976.
[27] Zhang Y., Zhong H., Belić M.R., Ahmed N., Zhang Y., Xiao M., *Diffraction-free beams in fractional Schrödinger equation*, Scientific Reports **6**(11), 2015, article no. 23645, DOI: 10.1038/srep23645.

[28] ZHANG L.F., LI C.X., ZHONG H.Z., XU C.W., LEI D.J., LI Y., FAN D.Y., *Propagation dynamics of super-Gaussian beams in fractional Schrödinger equation: from linear to nonlinear regimes*, Optics Express **24**(13), 2016, pp. 14406–14418, DOI: 10.1364/OE.24.014406.

[29] ZHANG Y., ZHONG H., BELIĆ M.R., Y. ZHU, ZHONG W., ZHANG Y., CHRISTODOULIDES D.N., XIAO M., *PT symmetry in a fractional Schrödinger equation*, Laser & Photonics Reviews **10**(3), 2016, pp. 526–531, DOI: 10.1002/lpor.201600037.

[30] LIEMERT A., KIENLE A., *Fractional Schrödinger equation in the presence of the linear potential*, Mathematics **4**(2), 2016, article no. 31, DOI: 10.3390/math4020031.

[31] SEGEV M., VALLEY G.C., BASHAW M.C., TAYA M., FEJER M.M., *Photovoltaic spatial solitons*, Journal of the Optical Society of America B **14**(7), 1997, pp. 1772–1781, DOI: 10.1364/JOSAB.14.001772.

[32] LU K., LI K., ZHANG Y., YUAN C., MIAO C., CHEN L., XU J., *Gray photorefractive polymeric optical spatial solitons*, Optics Communications **283**(23), 2010, pp. 4741–4748, DOI: 10.1016/j.optcom.2010.06.102.

[33] ZHANG T.H., REN X.K., WANG B.H., LOU C.B., HU Z.J., SHAO W.W., XU Y.H., KANG H.Z., YANG J., YANG D.P., FENG L., XU J.J., *Surface waves with photorefractive nonlinearity*, Physical Review A **76**(1), 2007, article no. 013827, DOI: 10.1103/PhysRevA.76.013827.

[34] MASOOD KHALIQUE C., BISWAS A., *A Lie symmetry approach to nonlinear Schrödinger's equation with non-Kerr law nonlinearity*, Communications in Nonlinear Science and Numerical Simulation **14**(12), 2009, pp. 4033–4040, DOI: 10.1016/j.cnsns.2009.02.024.

[35] YAN Y.Y., LIU W.J., ZHOU Q., BISWAS A., *Dromion-like structures and periodic wave solutions for variable-coefficients complex cubic–quintic Ginzburg–Landau equation influenced by higher-order effects and nonlinear gain*, Nonlinear Dynamics **99**(2), 2020, pp. 1313–1319, DOI: 10.1007/s11071-019-05356-0.

[36] BISWAS A., YILDIRIM Y., YASAR E., ZHOU Q., MAHMOOD M.F., MOSHOKOA S.P., BELIC M., *Optical solitons with differential group delay for coupled Fokas–Lenells equation using two integration schemes*, Optik **165**, 2018, pp. 74–86, DOI: 10.1016/j.ijleo.2018.03.100.

[37] BISWAS A., YILDIRIM Y., YAŞAR E., ZHOU Q., MOSHOKOA S.P., BELIC M., *Optical soliton solutions to Fokas-Lenells equation using some different methods*, Optik **173**, 2018, pp. 21–31, DOI: 10.1016/j.ijleo.2018.07.098.

[38] BISWAS A., EKICI M., SONMEZOGLU A., BELIC M.R., *Highly dispersive optical solitons with Kerr law nonlinearity by F-expansion*, Optik **181**, 2018, pp. 1028–1038, DOI: 10.1016/j.ijleo.2018.12.164.

Received February 28, 2022
in revised form April 20, 2022